Nondispersive Membrane Solvent Back Extraction of Phenol

Nondispersive back extraction of phenol from methyl isobutyl ketone into caustic solutions has been studied using microporous polymeric membranes in flat as well as hollow-fiber form. Dispersion-free reactive back extraction was successfully achieved using the correct phase pressure difference. The predictive capabilities of the mathematical models developed for such a system have been investigated. This study indicates that the overall mass transfer can be controlled by boundary layer resistance and/or the membrane transfer resistance, depending on the flow configuration, the nature of the membrane, and the regime of caustic concentration. Individual film transfer coefficients on the shell side and the tube side have been isolated for different hollow-fiber modules. A commercially available 15 cm long module containing hydrophobic microporous hollow fibers has provided very low values of height of transfer unit (HTU) and very high phenol recoveries. The experimentally obtained HTUs of this module have been predicted with significant accuracy.

R. Basu
R. Prasad
K. K. Sirkar
Department of Chemistry and
Chemical Engineering
Center for Membranes and
Separation Technologies
Stevens Institute of Technology
Castle Point, Hoboken, NJ 07030

Introduction

Inert, polymeric, microporous membrane-based dispersion-free extraction devices are increasingly being used as alternatives to liquid-liquid dispersion type extractors. Recent studies have used flat microporous hydrophobic membranes (Kiani et al., 1984; Prasad et al., 1986), flat microporous hydrophilic and composite hydrophilic-hydrophobic membranes (Prasad and Sirkar, 1987a,b), and microporous hydrophobic and hydrophilic hollow-fiber modules (D'Elia et al., 1986; Prasad and Sirkar, 1987a, 1988; Alexander and Callahan, 1987; Dekker et al., 1987; Dahuron and Cussler, 1988). Extraction with microporous hollow fibers (MHF) can provide high mass transfer rates per unit volume since hollow-fiber modules can pack an enormous surface area. The technique also overcomes many conventional liquid extraction shortcomings, for example, flooding limitations on independent phase flow rate variations, a requirement of density difference, and inability to handle particulates (Kiani et al., 1984; Frank and Sirkar, 1985, 1986; Prasad and Sirkar, 1988; Prasad et al., 1988).

Chemical reaction, often employed in liquid-liquid mass transfer processes, enhances the transport of the diffusing species. The reaction can be instaneous, fast, or slow and can be reversible or irreversible. An instantaneous chemical reaction is of great advantage because of the large enhancement of mass transfer coefficient and the increased concentration driving force (Grosjean and Sawistowski, 1980). Instantaneous chemical reaction has long been used for back extraction processes for removal of solute species such as phenol to free the solvent for reuse (Lanouette, 1977; Jauernik, 1960). Back extraction of phenol with caustic is also adopted in emulsion liquid membrane processes (Cahn and Li, 1974; Halwachs et al., 1980; Terry et al., 1982; Borwankar et al., 1988).

Solvent extraction with microporous membranes has wide dimensions. The membrane can be hydrophobic or hydrophilic; the instantaneous reaction front can be inside the membrane or in the film outside the membrane; there are preferred combinations of membrane wetting characteristics, phase in the membrane pore, and solute distribution coefficients. Maximization of mass transfer rate vis-a-vis these conditions is of intrinsic interest in nondispersive solvent extraction as well as in contained liquid membrane processes (Sengupta et al., 1988a,b) where two phase interfaces are immobilized, as opposed to just one in membrane solvent extraction. Further such studies will provide a quantitative basis for analyzing membrane-based

Correspondence concerning this paper should be addressed to K. K. Sirkar.
Present address of R. Prasad: Hoechst Celanese Inc., SPD, Charlotte, NC 28217.

multiphase reactors as well as membrane reactors as these are commercialized.

We have explored here the phenomenon of nondispersive solvent extraction in organic-aqueous systems with an instantaneous chemical reaction using microporous polymeric membranes. The nondispersive back extraction rate of phenol from methyl isobutyl ketone (MIBK) has been studied using various caustic solutions. Microporous polymeric membranes in flat and hollow fine-fiber form have been used. Flat membranes investigated include hydrophobic polypropylene, hydrophilic nylon 6, and hydrophobic-hydrophilic sandwiches. Hollow-fiber studies involved either hydrophobic membranes of polypropylene or hydrophilic membranes of nylon 6. The solute phenol was selected not only because it is a pollutant but also because of its behavioral similarity to bioactive solutes of relevance in the pharmaceutical industry.

Mass transfer accompanied by instantaneous chemical reaction can be described by a relatively simple mathematical model, particularly if the film theory assumption is applicable. Hatta originally developed a model for gas absorption with instantaneous chemical reaction (Astarita, 1967). It can be applied equally well to liquid-liquid systems (Grosjean and Sawistowski, 1980).

In nondispersive back extraction with instantaneous chemical reaction, the Hatta model has been extended here to a membrane-based reactive separation process by incorporating the additional membrane resistance wherever applicable. The effect of two regimes of NaOH concentration (stoichiometric excess or stoichiometric deficient) on mass transfer has been investigated. How the overall mass transfer can be controlled by boundary layer resistances and/or the membrane transfer resistance, depending on the nature of the membrane and the regime of NaOH concentration, has been explored. For hollow-fiber modules, the individual film transfer coefficients on the shell side and the tube side have been isolated by using excess caustic on the other side and have been compared with existing correlations. A practical illustration of this technique of back extraction has been studied by using a commercially available large surface area hydrophobic MHF module to achieve very high phenol recovery. The experimentally obtained height of transfer unit (HTU) values of this MHF module have also been compared with the theoretically calculated values.

Mathematical Models

In nondispersive microporous membrane-based solvent extraction without any chemical reaction, the overall mass transfer coefficient for the solute, K_o, has been expressed in terms of individual mass transfer resistances (Kiani et al., 1984; Prasad, 1986; Prasad and Sirkar, 1988) for various geometrical configurations and flow conditions. For illustration, we indicate here only two expressions for the local organic-phase-based overall mass transfer coefficient in MHF modules with the organic phase flowing in the shell side. Note that the hydrophobic membrane pores have the organic phase and the hydrophilic membrane pores have the aqueous phase; further, the phase excluded from the pores is at a higher pressure. In conventional aqueous-organic solvent extraction, there are only two resistances, the aqueous film and the organic film. In membrane solvent extraction the additional membrane resistance belongs to the resistance of that phase which occupies the membrane pores:

Hydrophobic MHF

$$1/K_o d_i = (1/k_{os} d_o + 1/k_{mo} d_{lm}) + (m_i/k_{wt} d_i) \quad (1)$$

Organic resistance | Aqueous resistance

Hydrophilic MHF

$$1/K_o d_o = (1/k_{os} d_o) + (m_i/k_{mw} d_{lm} + m_i/k_{wt} d_i) \quad (1a)$$

Organic resistance | Aqueous resistance

For a large m_i system (e.g., MIBK-water-phenol), the third term on the righthand side of Eq. 1 is dominant whereas in Eq. 1a the second and third righthand terms are dominant. Aqueous resistance dominates since phenol prefers the solvent MIBK at lower pH. Therefore, when $m_i \gg 1$, Eqs. 1 and 1a can respectively be simplified to:

$$1/K_o d_i \simeq m_i/k_{wt} d_i \quad (2)$$

$$1/K_o d_o \simeq m_i/k_{mw} d_{lm} + m_i/k_{wt} d_i \quad (2a)$$

Consider now the case for sufficient amount of caustic such

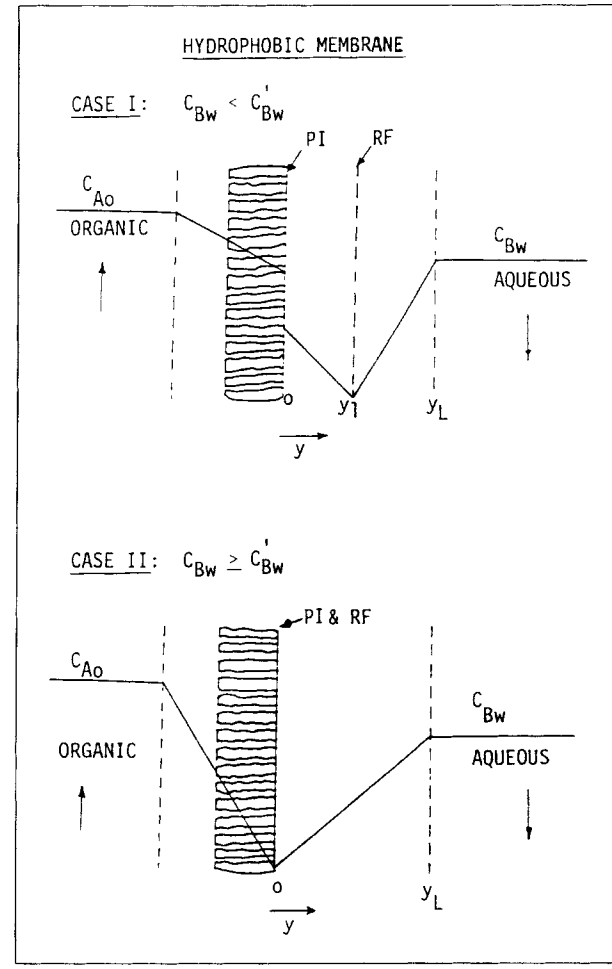

Figure 1. Film-theory concentration profiles for mass transfer with instantaneous chemical reaction.

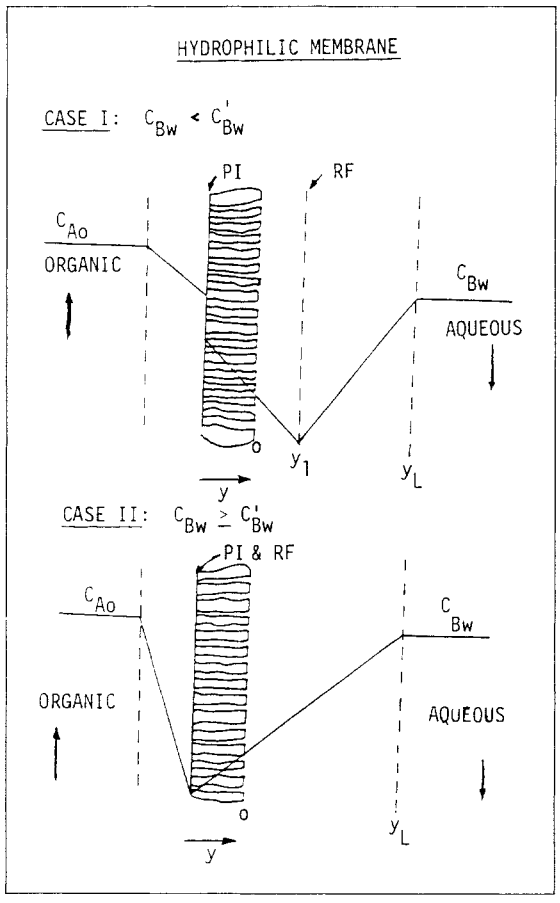

Figure 2. Film-theory concentration profiles for mass transfer with instantaneous chemical reaction.

that there is a reaction front (RF) and it is at the phase interface (PI); see Figures 1, 2, and 3. In such a case, for Eq. 1 the third term on the righthand side is absent; for Eq. 1a the second and third terms on the righthand side are absent. Thus, in a hydrophobic MHF membrane the aqueous film resistance, which was the controlling resistance for the nonreactive case for a large m_i system, is no longer present. In a hydrophilic hollow fiber with instantaneous chemical reaction at the phase interface, both the aqueous boundary layer resistance and the aqueous-filled membrane resistance have disappeared; only the organic boundary layer resistance is left. This case should provide the highest nondispersive mass transfer rate for an instantaneous chemical reaction with a microporous membrane.

Hatta (Astarita, 1967) modified the two-film mass transfer model during gas absorption to account for simultaneous chemical reaction and derived an expression for liquid phase mass transfer rate in the presence of an instantaneous irreversible chemical reaction. His treatment has been applied to nondispersive back extraction with instantaneous chemical reaction using microporous membrane by properly incorporating the membrane mass transfer resistance. Two cases are considered for each type of membrane: hydrophobic, Figure 1; hydrophilic, Figure 2; and composite, Figure 3:

Case I. The reaction plane is located in the film of aqueous phase so that, in addition to diffusing in the organic phase, phenol diffuses in the aqueous phase also from the phase interface to the reaction plane.

Case II. The phase interface forms the reaction plane so that phenol diffuses only in the organic phase. The process is controlled completely by resistance in the organic phase (in case of hydrophobic membrane, this will be the organic boundary layer plus the membrane phase).

Case II occurs if the concentration of sodium hydroxide (component B) is greater than (or equal to) its critical concentraction, C'_{Bw}, given by

$$C'_{BW} = (b/a)(D_{AW}/D_{Bw})(k_o/k_w)\, C_{Ao} \tag{3}$$

where a, b are stoichiometric coefficients (= 1 in the present case), C is the molar concentration, and subscript A denotes phenol. Here k_o may include the hydrophobic membrane phase and k_w may include the hydrophilic membrane phase.

In case I, the flux of phenol is given by

$$N_A = K_o(C_{Ao} + (a/b)(D_{Bw}/D_{Aw})\, C_{Bw}) \tag{4}$$

where, for a hydrophobic film (organic in pore)

$$1/K_o = 1/k_o + 1/k_{mo} + m_i/k_w \tag{5}$$

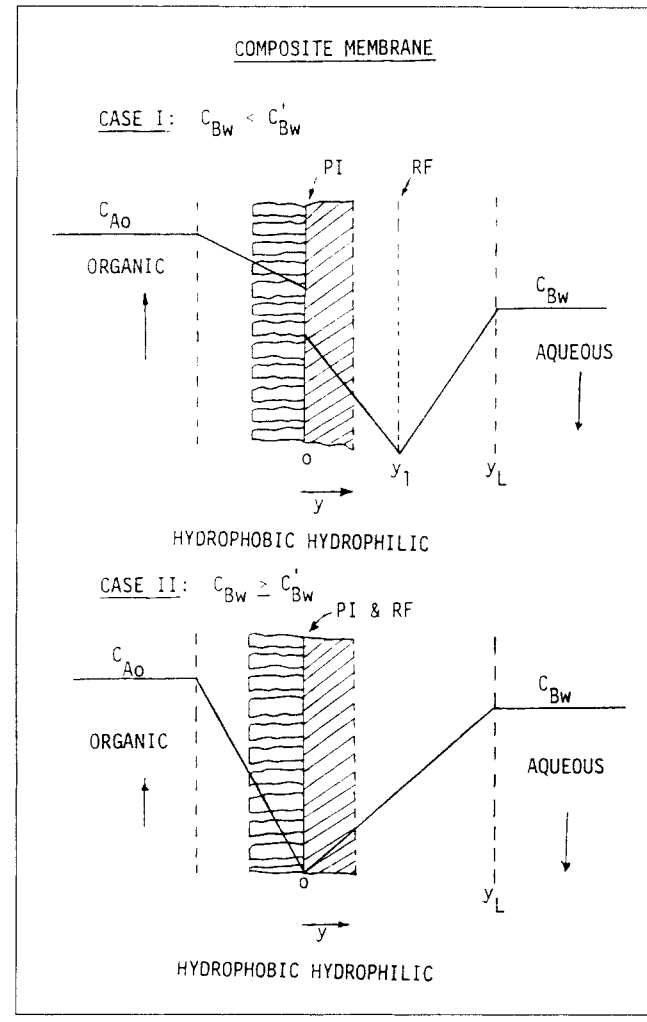

Figure 3. Film-theory concentration profiles for mass transfer with instantaneous chemical reaction.

for a hydrophilic film (water in pore)

$$1/K_o = 1/k_o + m_i/k_{mw} + m_i k_w \tag{6}$$

and for a composite film (organic-hydrophobic:water-hydrophilic)

$$1/K_o = 1/k_o + 1/k_{mo} + m_i/k_{mw} + m_i/k_w \tag{7}$$

In case II, the flux of phenol across the interface is given by

$$N_A = K_o C_{Ao} \tag{8}$$

where, for a hydrophobic film (organic in pore)

$$1/K_o = 1/k_o + 1/k_{mo} \tag{9}$$

for a hydrophilic film (water in pore)

$$1/K_o = 1/k_o \tag{10}$$

for a composite film (organic-hydrophobic:water-hydrophilic)

$$1/K_o = 1/k_o + 1/k_{mo} \tag{11}$$

In Eqs. 5–7 and 9–11, the diameter effect needed for hollow fibers is absent.

So far we have dealt with local flux expressions. Flat polymeric membranes of small surface area can be employed to verify such a model. However, for MHF modules and for deficient caustic, the bulk NaOH concentration changes along the length of the module. The location where caustic concentration becomes zero is denoted by A_p^*. Therefore we must solve the system of differential equations shown below for *cocurrent flow:*

From $A^* = 0$ to $A^* = A_p^*$,

$$dC_{Ao}^*/dA^* = -(K_o A_t/Q_{org}) \cdot (C_{Ao}^* + m_i(D_{Bw}/D_{Aw})C_{Bw}^*) \tag{12}$$

$$dC_{Bw}^*/dA^* = -(K_o A_t/Q_{aq}) \cdot (C_{Ao}^* + m_i(D_{Bw}/D_{Aw})C_{Bw}^*) \tag{13}$$

At

$$A^* = 0,\ C_{Ao}^* = 1,\ C_{Bw}^* = C_{Bw}^o/C_{Ao}^o \tag{14}$$

From $A^* = A_p^*$ to $A^* = 1$,

$$dC_{Ao}^*/dA^* = -(K_o A_t/Q_{org})(C_{Ao}^* - m_i C_{Aw}^*) \tag{15}$$

$$dC_{Aw}^*/dA^* = (K_o A_t Q_{aq})(C_{Ao}^* - m_i C_{Aw}^*) \tag{16}$$

At

$$A^* = A_p^*,\ C_{Ao}^* = C_{Ao}^{p*},\ C_{Aw}^* = 0 \tag{17}$$

Here

$$C_{Ao}^* = C_{Ao}/C_{Ao}^o,\ C_{Bw}^* = C_{Bw}/C_{Ao}^o,\ C_{Aw}^* = C_{Aw}/C_{Ao}^o,\ A^* = A/A_t \tag{17a}$$

Performance of commercially available large surface area MHF modules can be judged using the HTU concept (Prasad and Sirkar, 1988; Prasad et al., 1988), since HTU values illustrate the efficiency of contacting. HTU is defined as

$$HTU = Q_{org}/(K_o a \times \text{empty shell cross-sectional area}) \tag{18}$$

or

$$HTU = Q_{eq}/(K_w a \times \text{empty shell cross-sectional area}) \tag{19}$$

depending on whether the overall K is based on the organic film or the aqueous film. These values were calculated based on the actual hollow-fiber interfacial area per unit volume, a, of the modules in the present study. Note that K_o or K_w in Eq. 18 or 19 is an average value over the whole module.

Experimental Method

Chemicals and materials

All chemicals were used as received. The solvent, methyl isobutyl ketone, was certified ACS grade (Fisher Scientific, Fairlawn, NJ). Puriss p.a. grade phenol loose crystals were obtained from Fluka Chemical Corporation, Ronkonkoma, NY. Sodium hydroxide was certified ACS grade (Fisher Scientific). Acetonitrile was HPLC grade (Fisher Scientific). Orthophosphoric acid was HPLC grade (Fisher Scientific). Oxalic acid dihydrate was Fisher certified reagent. 4-amino-antipyrin was purum grade from Fluka. Potassium ferricyanide was analytical reagent (Mallinckrodt, Paris, KY). Sodium borate decahydrate was Baker analyzed reagent (J.T. Baker Chemical Co., Phillipsburg, NJ).

For flat microporous membrane studies we used Celgard 2400 (hydrophobic polypropylene, Hoechst Celanese Separations Products Division, Charlotte, NC) and nylon 6 (hydrophilic membranes, ENKA America Inc., Technical Membrane Group, Asheville, NC). Their physical properties are given in Table 1. For microporous hollow fiber (MHF) studies, we used modules containing either polypropylene hollow fibers (hydrophobic) or nylon 6 hollow fibers (hydrophilic). Polypropylene hollow fibers were X-20 (240 μm ID, 25 μm wall thickness) or X-10 (100 μm ID, 25 μm wall thickness) obtained from Hoechst Celanese Separations Products Division, Charlotte, NC. Nylon 6 (polyamide PA6) hollow fibers were from Enka America Inc., Asheville, NC. Details are given in Table 1.

The hollow-fiber modules, Table 2, resemble a shell-and-tube heat exchanger. The shell of modules 1 and 2 consisted of 6.25 mm OD stainless steel tubes with 6.25 mm male run tees at each end of the shell (Prasad and Sirkar, 1988). The fibers were epoxy potted at the end of the male run tees. For hydrophobic module 1, a solvent-resistant epoxy with an activator (Beacon Chemicals, Mt. Vernon, NY) was used. For hydrophilic module 2, we used another solvent-resistant epoxy with a different activator. Both epoxys have been found to be organic solvent and caustic resistant. We also used a high surface area hydrophobic Liqui-Cell MHF module 3 (surface area 2,827 cm^2 based on OD), for high phenol recovery. The details of this module are given in Table 2.

Analytical procedures

Aqueous sodium hydroxide concentration was measured by titration against standard oxalic acid using phenolphthalein as

Table 1. Physical Properties* of Membranes Used

Flat Membrane	Material	Pore Size μm	Thickness μm	Porosity	Bubble Point** Bar
Celgard 2400 (hydrophobic)	Polypropylene	0.02	25.4	0.38	>6.89†
Nylon 6 (hydrophilic)	Polyamide 6	0.2	110	0.7	min. 3.75 max. 4.65

Hollow-Fiber Membrane	Material	Pore Size μm	OD μm	ID μm	Porosity	Bubble Point** Bar
Celgard X-20 (hydrophobic)	Polypropylene	0.03	290	240	0.4	10.34
Nylon 6 (hydrophilic)	Polyamide 6	0.2	1,000	600	0.75	3.7
Celgard X-10 (hydrophobic)	Polypropylene	0.03	150	100	0.2	10.34

*From manufacturer's catalog
**Against water
†Callahan (1988)

indicator. Organic phase (MIBK) phenol concentration was measured in an HP 1090 liquid chromatograph using a Hypersil ODS (5 μm) Chromsep analytical HPLC column. The filter photometric detector was set at 280 nm. The mobile phase was acetonitrile (35%)–water (65%) at a flow rate of 0.2 cm^3/min. The organic samples were diluted 1:2 with acetonitrile to get better resolution of peaks.

Alkaline phase phenol concentration, in the range 0 to 150 mg/L phenol, was measured by a spectrophotometer (Spectronic 1001, Bausch and Lomb), setting the detector at the optimum wavelength of 520 nm. For this, a 0.5 mL aliquot of alkaline phenol solution was diluted by adding 15.0 mL of buffered reagent solutions, which consisted of 5.0 mL of one solution (4.767 g sodium borate 10-hydrate, 0.352 g sodium hydroxide, and 0.06 g 4-amino-antipyrine in 1L distilled water) and 10.0 mL of a second solution (4.767 g sodium borate 10-hydrate, 0.352 g sodium hydroxide, and 0.15 g potassium ferricyanide in 1 L distilled water) (Cooney and Jin, 1985).

At a higher concentration of phenol, a method was developed for analyzing alkaline phenol samples by HPLC. The alkaline phenol samples were diluted by aqueous ortho-phosphoric acid (made by diluting 85% HPLC grade ortho-phosphoric acid in double-distilled water). The aqueous phosphoric acid concentration was maintained such that the pH of the phenol samples was close to 7.0. The HPLC column, mobile phase, and detector wavelength were the same as those for the organic phase phenol analysis. This method of analysis showed very good reproducibility.

Table 2. Hollow-Fiber Module Details

Membrane	Shell	No. of Fibers	Length cm	Shell-side Void Frac.	a† cm^{-1}
Celgard X-20	0.46 cm ID S.S. tube*	102	18.5	0.59	46.8
Nylon 6	0.46 cm ID S.S. tube**	10	7.0	0.52	11.5
Celgard X-10	1.9 cm ID Nylon tube***	4,000	15.0	0.75	44.7

†Based on ID of Fiber.
*Module 1, surface area 142.28 cm^2
**Module 2, surface area 13.19 cm^2
***Module 3, surface area 1884.96 cm^2, Liqui-Cel, Cat. No. 35554-10A, Hoechst Celanese SPD, NC.
All surface areas are based on ID of fibers.

Experimental setup and procedures

For the flat membrane studies we used a test cell and flow loop similar to that used by Kiani et al. (1984). The only modification was to introduce two check valves at the reservoir outlets of feed and extractant so that, in case of any pressure imbalance or membrane failure, one fluid could not mix with the other fluid in the reservoirs (Prasad et al., 1986). The phase with higher pressure was kept on the top side of the test cell (Kiani et al., 1984; Prasad, 1986). Phenol concentration in feed MIBK was 0.1 M.

For microporous hollow-fiber modules we used a flow loop similar to that used by Prasad and Sirkar (1988). Here too we introduced check values at the outlet of the feed and extractant reservoirs. The hydrophobic MHF modules were operated with the aqueous phase at a higher pressure than the organic phase. Experiments were done with the aqueous phase flow on the tube side (organic flow on the shell side) as well as with the aqueous flow on the shell side (organic flow on the tube side). Care was taken to ensure that the aqueous phase pressure was greater than the organic phase pressure at every location of the permeator. In the case of hydrophilic MHF modules, the organic phase was always kept at a pressure higher than the aqueous phase pressure (Prasad and Sirkar, 1988). Again, experiments were done with the organic phase on the shell side (aqueous phase on tube side) as well as with organic phase on tube side (aqueous phase on shell side). In all MHF experiments the flow of the phases (organic and aqueous) was *cocurrent*.

The overall mass transfer coefficients were calculated using the relations given by Prasad and Sirkar (1988). The membrane resistances were calculated using the relations

$$k_{mw} = D_{Aw}\epsilon_m / t\tau_m \tag{20}$$

$$k_{mo} = D_{Ao}\epsilon_m / t\tau_m \tag{21}$$

In the case of hollow fibers, $t = (d_o - d_i)/2$. The membrane porosity and thickness were obtained from the manufacturer's information. The diffusion coefficient of phenol was calculated using the Wilke and Chang (1955) equation. The diffusion

coefficient of NaOH in water was obtained from *International Critical Tables* (1929). The phenol distribution coefficient m_i between MIBK and water has been reported by Won and Prausnitz (1975) and Prasad and Sirkar (1988). The tortuosities of hydrophobic membranes were taken from Prasad et al. (1986), Prasad and Sirkar (1987b, 1988), and Sengupta et al. (1988b). The tortuosities of hydrophilic nylon 6 membranes are not available in the literature and they were not needed for our calculations.

Results and Discussion

We report first the values of overall mass transfer coefficients for phenol extraction from aqueous phase to methyl isobutyl ketone (MIBK) without any reaction. These overall mass transfer coefficient data were needed to verify the caustic-deficient model. Some mass transfer coefficient data for the MIBK-water-phenol system using Celgard 2400 flat membrane and Celgard X-20 hollow fibers are also reported in literature (Prasad, 1986; Prasad and Sirkar, 1988). It is to be noted that we have presented the overall mass transfer coefficient as K_o, not as K_w. For a large m_i system, it is customary to express K as K_w, since the major mass transfer resistance is in the aqueous region. However, for our model prediction we needed the overall mass transfer coefficient in the K_o form.

We next present the mass flux of phenol in back extraction with deficient caustic for both flat and MHF membranes, along with the predicted values. We then illustrate the mass transfer coefficients K_o obtained by using excess caustic for one and two flat membranes. The data were used to demonstrate how the controlling mass transfer resistance had been shifted from that in simple nonreactive extraction studies. We have thereafter isolated shell-side and tube-side Sherwood numbers for MHF modules using excess caustic (after subtracting the membrane phase resistance wherever applicable) and compared those with values from available correlations. We have in the end reported very high recovery of phenol into the aqueous phase using a Liqui-Cel hydrophobic MHF module with large surface area and have compared the experimentally obtained HTU values with those predicted by the model.

Figure 4 shows the experimentally obtained overall phenol mass transfer coefficients for hydrophobic, hydrophilic, and

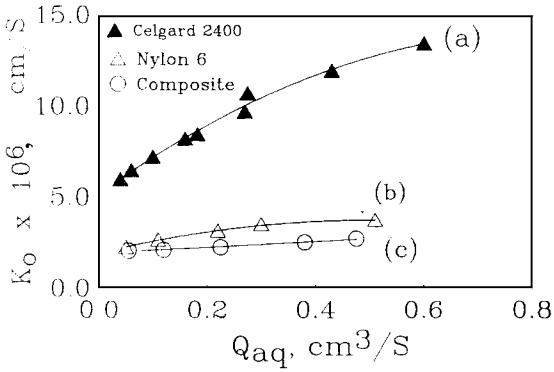

Figure 4. Extraction of phenol from water into MIBK using flat membranes.

Contact area 13.37 cm^2
(a) Hydrophilic Celgard 2400
(b) Hydrophobic nylon 6
(c) Composite, Celgard 2400 + nylon 6

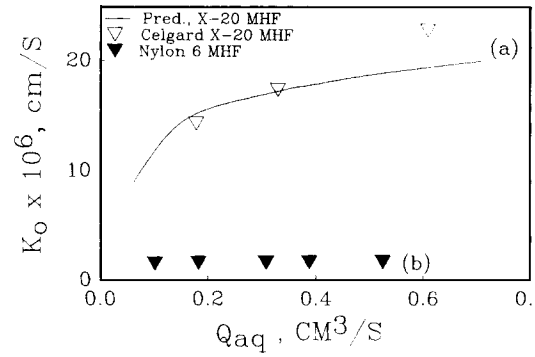

Figure 5. Extraction of phenol from water into MIBK using MHF modules.

(a) Hydrophobic MHF module 1, Celgard X-20
(b) Hydrophilic MHF module 2, nylon 6

composite flat membranes. Figure 5 shows the overall mass transfer coefficients for phenol extraction using hydrophobic MHF module 1. The solid line in the plot represents the predicted overall mass transfer coefficients. In this MHF module experiment, aqueous phase was flowing in the tube side (organic phase on shell side). For predicting the overall mass transfer coefficient, we have used the Graetz solution (Skelland, 1974) for tube-side boundary layer resistance as recommended by Prasad and Sirkar (1988). We have used the correlation of Prasad and Sirkar (1988) for shell-side boundary layer resistance, and a tortuosity factor for membrane phase resistance as reported by Prasad and Sirkar (1988). All these individual resistances were combined, incorporating the diameter effect indicated by Eq. 1. Figure 5 also shows the experimental overall mass transfer coefficients for nylon 6 MHF module 2 (organic phase on shell side). ΔC_{LM} was used to determine all experimental K_o values in Figure 5.

Using Eq. 3 and the appropriate mass transfer coefficient and diffusion coefficient values, the critical caustic concentration, C'_{Bw}, necessary to run back extraction experiments at the two regimes of caustic concentration was obtained. For the flow conditions employed and an organic phase phenol concentration of 0.1 M, a caustic concentration less than 0.025 M was found to lead to the deficient caustic regime for a hydrophobic membrane; for a hydrophilic membrane, the corresponding caustic concentration is 0.075 M. We did not estimate the critical caustic concentration for a composite membrane since it will be higher than 0.075 M. These critical concentration values are to be taken as rule-of-thumb values; working with a caustic concentration much lower than this value will definitely provide the deficient caustic regime.

To operate in the deficient caustic regime, we therefore used for hydrophobic membranes a caustic concentration of 0.01 M; for hydrophilic and composite membranes we used 0.05 M caustic. Figures 6a, b, and c show the experimental data points and the predicted curves for phenol flux using the model for, respectively, hydrophobic, hydrophilic, and composite flat membranes. For predicting the fluxes we used the mass transfer coefficient values from Figure 4. While the experimental values match well with the model predictions for hydrophobic and hydrophilic flat membranes, the composite membrane model predicts about 15% higher flux than that observed over the whole flow rate range. Unequal amounts of aqueous phase

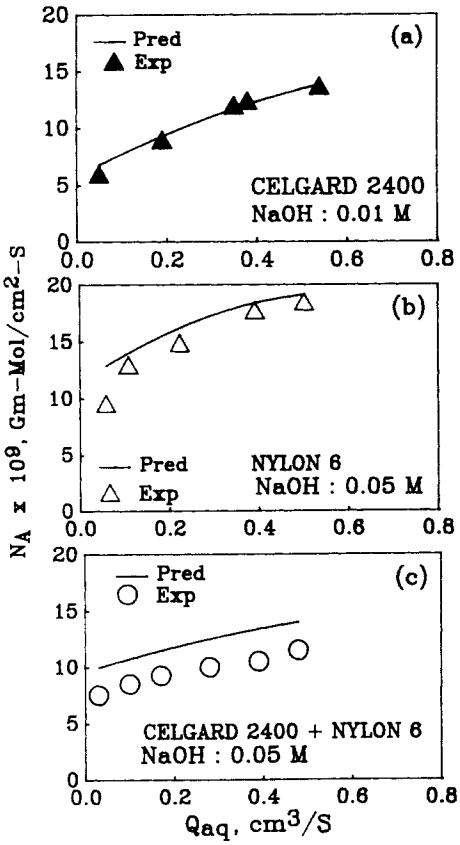

Figure 6. Extraction of phenol from MIBK into stoichiometrically deficient caustic.

Contact area 13.37 cm^2
(a) Hydrophobic Celgard 2400
(b) Hydrophilic nylon 6
(c) Composite, Celgard 2400 + nylon 6

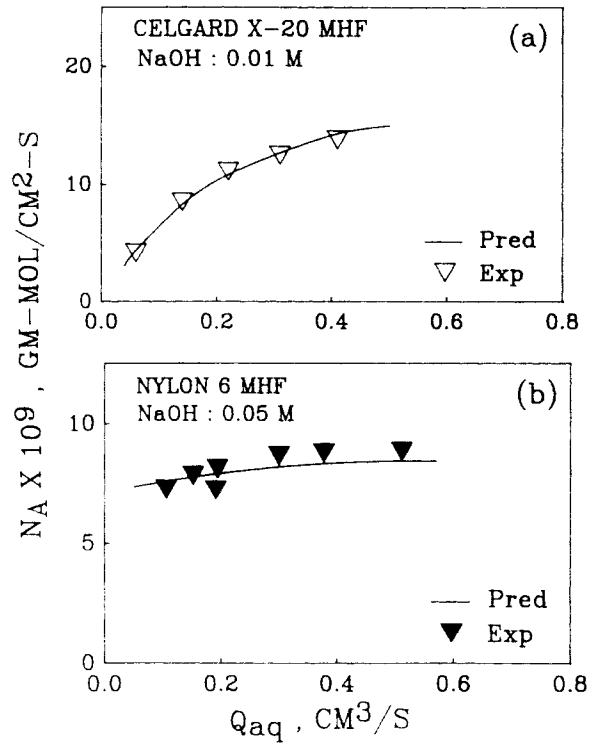

Figure 7. Extraction of phenol from MIBK into stoichiometrically deficient caustic.

(a) Hydrophobic MHF module 1, Celgard X-20
(b) Hydrophilic MHF module 2, nylon 6

sandwiched between the two membranes for two different sets of experiments (extraction and back extraction) probably is the source of this difference.

What is the basis for suggesting that an aqueous (but not an organic) film is trapped between the two membranes? Nylon 6 hydrophilic membranes have relatively large pore size (0.2 μm). Even though they are preferentially wetted by the aqueous phase, the organic phase can also enter into the pores of this membrane at relatively small values of excess organic phase pressure. Although previous work (Prasad and Sirkar, 1987b) suggests that dispersion-free operation can be achieved with composite membranes with either phase at a higher pressure, it was useful in our case to keep the aqueous phase at a higher pressure to ensure that the aqueous phase was actually inside the pores of nylon 6 membrane. This justifies our presumption that the trapped liquid film is aqueous. For a high m_i system this trapped aqueous film can offer a significant mass transfer resistance.

We also carried out deficient caustic experiments using hydrophobic MHF module 1 and 0.01 M caustic. In these experiments the aqueous phase flow was on the tube side. The model prediction was done by solving the system of differential Eqs. 12 to 13 and Eqs. 15 to 16 with the initial conditions of Eqs. 14 and 17, using the IMSL routine DVERK. In this calculation we used for K_o the predicted nonreactive mass transfer coefficients shown in Figure 5. Figure 7a shows the experimental average flux data at various aqueous flow rates; the solid line in the figure shows the model prediction. They agree quite well.

Deficient caustic experiments were also done using hydrophilic nylon 6 MHF module 2 and 0.05 M caustic. Here too the aqueous phase flow was in the tube side of the module. Model prediction was done in a fashion similar to that for the hydrophobic module; we used the nonreactive mass transfer coefficient data of Figure 5. Figure 7b shows the experimental data and model prediction of phenol fluxes for the hydrophilic MHF module. Figures 5 and 7b both show an almost flat mass transfer coefficient and mass flux as the aqueous flow rate is changed. High membrane wall thicknesses (200 μm) of hydrophilic nylon MHFs make the membrane phase resistance dominant, leading to the essentially flat nature of fluxes.

The variation of the mass transfer coefficient K_o with aqueous flow rate is shown in Figure 8 for one and two hydrophobic flat membranes and sufficient caustic (0.25 M). Observe that K_o remains essentially constant with aqueous flow variation. This is not surprising since, in the presence of sufficient caustic the aqueous boundary layer resistance is nonexistent. For comparison, we show the plot of K_w vs. Q_{aq} for a water run in the inset of Figure 8. It shows how the mass transfer coefficient varies with variation of aqueous flow rate for the nonreactive case. From the K_o values of one-membrane and two-membrane experiments in Figure 8, the membrane resistance can be evaluated.

Figure 9 shows K_o vs. Q_{aq} for one and two hydrophilic nylon 6 membranes and sufficient caustic (0.25 M). Here too the inset shows the K_w vs. Q_{aq} plot for the nonreactive water run (one nylon 6). Observe that K_o does not vary with Q_{aq} for the reactive

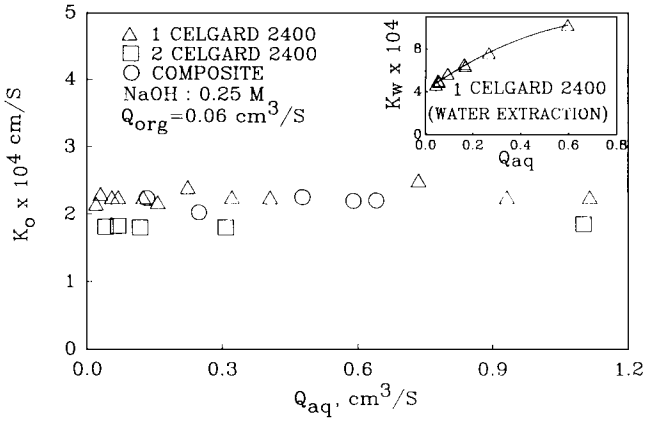

Figure 8. Effect of aqueous phase flow variation on extraction of phenol from MIBK into stoichiometrically sufficient caustic using hydrophobic and composite (Celgard 2400 + nylon 6) flat membranes.

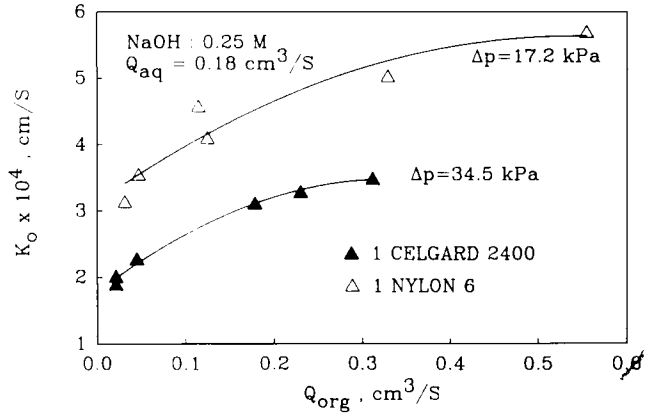

Figure 10. Effect of organic phase flow variation on extraction of phenol from MIBK into stoichiometrically sufficient caustic using either hydrophobic or hydrophilic flat membrane.

case. The figure also shows that using one or two membranes did not affect K_o; there is sufficient amount of caustic and the membrane pores are filled with aqueous phase such that the reaction interface is at the phase interface.

Figure 8 also illustrates K_o vs. Q_{aq} for the composite membrane. It can be seen that in case of interfacial reaction due to sufficient caustic, the presence of the hydrophilic membrane does not give rise to any additional mass transfer resistance. This is predicted by Eq. 11. In Figure 10, we have plotted K_o vs. Q_{org} separately for the hydrophilic and hydrophobic flat membranes for sufficient caustic. While Prasad (1986) showed that for Celgard 2400 K_w remains essentially constant with organic flow variation (large m_i system), here—due to interfacial chemical reaction—the mass transfer controlling resistance has shifted to the organic phase side and K_o varies with Q_{org}. A look at Eqs. 9 and 10 shows an extra membrane resistance ($1/k_{mo}$) with a hydrophobic film; therefore, in Figure 10, K_o for Celgard 2400 is less than that for nylon 6.

An instantaneous reaction at the phase interface when sufficient caustic is present then leads to elimination of aqueous resistance; we can use the same strategy with MHF modules to determine the Sherwood numbers N_{Sh} for the shell side and the tube side. Note that in the case of hydrophilic MHFs the overall mass transfer resistance will reflect only the boundary layer resistance on either side; for hydrophobic MHFs the overall mass transfer resistance will be the combined resistances of the membrane and the boundary layer on either side. Therefore, for hydrophobic MHFs the membrane resistance, determined by using the literature value of tortuosity (Prasad and Sirkar, 1988) and Eq. 21, was subtracted from the overall mass transfer resistance (including the diameter effect) to determine the shell-side or tube-side N_{Sh}.

Figure 11 shows the tube-side Sherwood number vs. tube-side Graetz number N_{Gz} (organic phase flow on tube side) data for hydrophobic module 1 and hydrophilic module 2. The solid line is the corresponding Graetz solution (Prasad and Sirkar, 1988). The Graetz solution for mass transfer in cylindrical tubes is the closed form solution of the parabolic differential equation for developed parabolic velocity profile, developing concentration profile, and constant wall concentration. The only difference

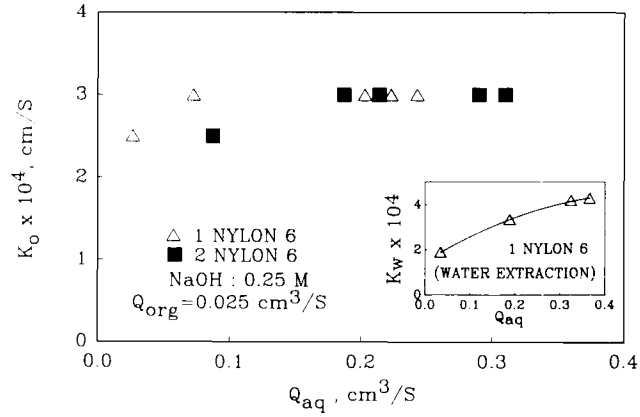

Figure 9. Effect of aqueous phase flow variation on extraction of phenol from MIBK into stoichiometrically sufficient caustic using hydrophilic flat membrane. ΔP = 20.7 kPa

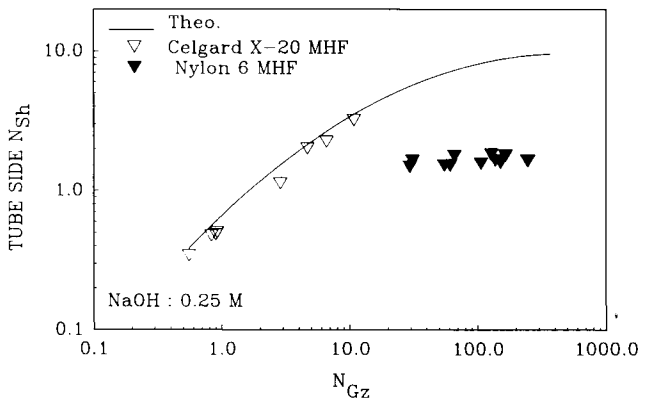

Figure 11. Tube-side N_{Sh}.
(a) Hydrophobic MHF module 1, Celgard X-20, avg. ΔP = 13.8 kPa
(b) Hydrophilic MHF module 2, nylon 6, avg. ΔP = 1.7–3.4 kPa

between our experimental conditions and the Graetz problem is that the membrane wall (inside) concentration is not constant. However, for this small MHF module 1, the solute recovery is limited; thus the wall concentration along the length does not change much, which explains why our experimental N_{Sh} values are close to those from the Graetz solution.

In a similar fashion, we determined the shell-side N_{Sh} for hydrophobic MHF module 1. Figure 12 shows the shell-side N_{Sh} vs. N_{Re} data for this module. The experimental points show that N_{Sh} follows a $N_{Re}^{0.6} N_{Sc}^{0.33}$ relationship as in Prasad and Sirkar (1988). But comparison with the correlation by Prasad and Sirkar shows that the present N_{Sh} is about 3 to 3.5 times higher. The correlation by Yang and Cussler (1986) is lower by almost as much. The reasons for this discrepancy are probably the following. The packing fractions of the hollow-fiber modules used to develop the shell-side correlations of Prasad and Sirkar (1988) were less than 0.20. Although they had made a few experiments with a module of larger packing fraction (0.40), these results were used only to demonstrate the very low HTU possible. There is considerable room for bypassing, channeling, and similar effects in the shell side of such modules. Thus the shell-side mass transfer behavior will vary widely from module to module. That there is a possibility of channeling on the shell side of these modules has also been suggested by Yang and Cussler (1986). Perhaps the extent of channeling in the densely packed module of this work is much less, resulting in a much higher transfer coefficient.

Figure 12 also illustrates the shell-side N_{Sh} vs. N_{Re} obtained similarly for the hydrophilic nylon 6 MHF module 2. Here also we see that N_{Sh} follows a $N_{Re}^{0.6} N_{Sc}^{0.33}$ relation. Further, for this module the data match well with the Prasad and Sirkar (1988) correlation for the shell side. Figure 12 also shows the N_{Sh} values using the correlation by Yang and Cussler (1986). We would like to note an unusual behavior of the hydrophilic nylon 6 MHFs. With the organic phase on the shell side and aqueous phase on the tube side and in the membrane pores, we have operated this MHF module up to a maximum pressure differential of 68.9 kPa (organic phase at higher pressure). Under these conditions we did not observe any phase breakthrough. If, however, the organic phase flows on the tube side (aqueous phase on the shell side and in the pores), phase breakthrough could be prevented only when the pressure differential did not exceed 1.72 to 3.45 kPa (organic phase at a higher pressure). Operating with a higher organic phase pressure caused organic phase breakthrough into the aqueous side; stable dispersion-free operation was no longer possible (keeping the organic phase at a lower pressure than the aqueous phase always caused aqueous phase breakthrough into the organic phase).

While working with the organic phase on the tube side, if the organic phase pressure exceeded 1.72–3.45 kPa the organic phase would go into the micropores of the hydrophilic MHFs. Dekker et al. (1987) have reported penetration of water into the micropores for large pore (0.1 μm) hydrophobic polypropylene fibers. This behavior most likely explains the tube-side experimental data for N_{Sh} for hydrophilic module 2 shown in Figure 11. Since the Graetz solution fitted well with our experimental tube-side N_{Sh} data obtained in hydrophobic MHF modules and small pore hydrophilic fiber modules (Prasad and Sirkar, 1988), we expected that it would be true for the large pore nylon 6 hydrophilic MHF module 2 also. Instead, the N_{Sh} was found to be much lower than that obtained from the Graetz solution and the experimental N_{Sh} was essentially independent of N_{Gz}. We suspect that organic phase penetrated inside the micropores and led to this lowered and flat N_{Sh}.

Why did the same phenomenon fail to occur when organic phase flow was on the shell side? Is it possibly due to the asymmetric nature of the membrane wall? Electronmicrographs of the inside, outside, and interior of the nylon hollow-fiber membrane wall were taken. Although the manufacturer reports a nominal pore size of 0.2 μm, we have observed many pores of 1 μm and above on both surfaces. The interior of the membrane appears to be more porous and to have larger pore size. It is difficult to assert that the membrane is definitely asymmetric. More important, when the organic phase is at a higher pressure on the shell side, the membrane wall is compressed, leading possibly to a pore size reduction. This would increase the magnitude of the breakthrough pressure. On the other hand, if the higher pressure organic phase is on the tube side, the membrane wall is distended; the pore sizes are enlarged, leading to a lower level of the breakthrough pressure. The very high porosity (~0.75) of the nylon material directly contributes to this behavior.

Figure 13 shows the enhancement factors, defined as N_A (with

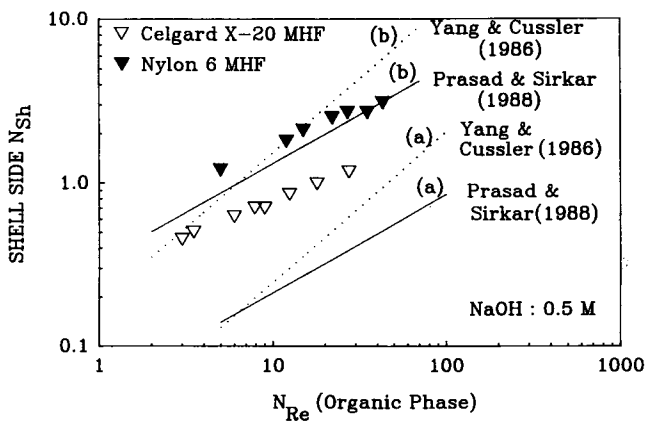

Figure 12. Shell-side N_{Sh}.

(a) Hydrophobic MHF module 1, Celgard X-20, avg. $\Delta P = 20.7$ kPa

(b) Hydrophilic MHF module 2, nylon 6, avg. $\Delta P = 13.8$ kPa

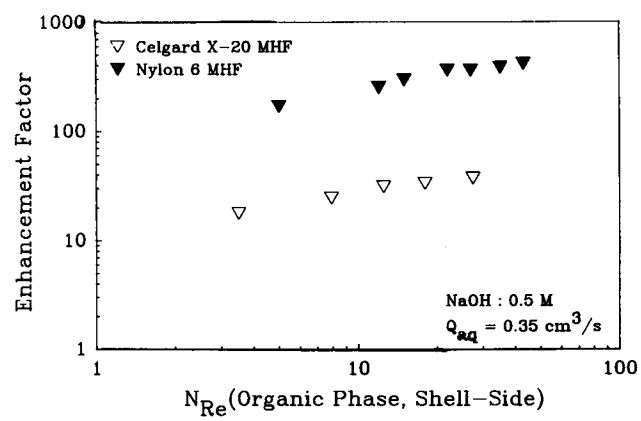

Figure 13. Enhancement factor.

(a) Hydrophobic MHF module 1, Celgard X-20

(b) Hydrophilic MHF module 2, nylon 6

Table 3. Percent Removal of Phenol and HTU for High Surface Area Celgard X-10 MHF Module 3

Q_{org}	Removal	HTU*, m	
cm^3/s	%	Exp.	Theory
0.07	99.85	0.083	0.082
0.14	98.08	0.082	0.091
0.25	89.31	0.105	0.105
0.41	72.39	0.140	0.124
0.59	58.44	0.170	0.145

$Q_{aq} = 0.28\ cm^3/s$; $C^o_{Ao} = 0.099 \times 10^{-3}\ mol/cm^3$.
Contact area (based on OD) = 2,827.43 cm^2
*Eq. 18 used to calculate HTU; $1/K_o d_o = 1/k_{os} + 1/k_{mo}d_o$ expression used for theoretical HTU.

reaction)/N_A (without reaction), for hydrophobic module 1 and hydrophilic module 2 at various organic phase flow rates. When there is no reaction, the aqueous phase membrane resistance is present in a hydrophilic membrane and the organic phase membrane resistance in a hydrophobic membrane. With reaction under stoichiometric excess NaOH, hydrophilic pore resistance disappears but it does not disappear in a hydrophobic membrane. Hence the relative increase in enhancement factors for the hydrophilic MHF vis-a-vis the hydrophobic MHF. Since the organic phase controls mass transfer under stoichiometric excess of NaOH, the enhancement factor increases as the organic phase resistance decreases. One could generate additional hypothetical curves by parametric variation of D_A/D_B.

We have also investigated the practical use of this technique for back extraction, for a large m_i system, by using a commercially available high surface area hydrophobic MHF module 3 described in Table 2. In this experiment, the organic phase was on the tube side. Table 3 shows a very high percentage removal of phenol from a 0.1 M organic feed for different organic flow rates. The NaOH concentration was 0.5 M and the aqueous flow rate was kept constant. The HTU of this module was experimentally determined as well as theoretically calculated using Eq. 18. For K_o needed in theoretical calculation of HTU, we used the Graetz solution for the tube-side coefficient and Eq. 21 for the membrane resistance (membrane parameters from Table 1 and tortuosity of X-10 microporous hollow fiber from Sengupta et al., 1988b). Table 3 shows the experimental and theoretical HTU values at different organic flow rates. It is evident that the theoretical HTU values are quite close to the experimentally obtained values at all organic flow rates.

We would like to indicate that throughout this study K_o values were calculated from the mass transfer rate using ΔC_{LM} values. However, the K_o expression from the Graetz solution used here (Skelland, 1974) is based on the arithmetic average concentration driving force ΔC_{AM}. Therefore, for the tube-side N_{Sh} calculations with module 1 and module 2, Figure 11, and for the HTU calculations with module 3, Table 3, ΔC_{AM} was used. The close correspondence between the experiment and the model for HTU prediction in a system with an instantaneous reaction is gratifying.

Conclusions

This work provides extensive data on nondispersive back extraction of phenol from MIBK to caustic solutions using microporous polymeric membranes with different wetting tendencies in flat and hollow fine-fiber form. The study indicated that the overall mass transfer enhanced by reaction can be controlled by boundary layer resistances and/or the membrane transfer resistance, depending on the flow configuration, the nature of the membrane, and the regime of NaOH concentration. Mathematical models developed for different types of membranes predict well the enhanced rate of phenol back extraction with instantaneous chemical reaction in the aqueous phase for two regimes of NaOH concentration: stoichiometric excess or deficient.

Chemically resistant hydrophilic hollow fine fibers with high porosity and low pore size are likely to provide an extremely high mass transfer rate in large m_i systems in the presence of an instantaneous chemical reaction. In spite of the additional membrane resistance, hydrophobic hollow fine fibers are almost equally attractive. A highly packed 15 cm long hydrophobic MHF module had provided very low HTU values and a very high phenol recovery. The experimentally obtained HTU of this MHF module has been predicted with significant accuracy. Existing correlations for shell-side mass transfer coefficient do not describe the measured values in a highly packed hydrophobic MHF module, suggesting the need for additional investigations. Stable nondispersive extraction for large pore hydrophilic nylon 6 hollow fibers with the organic phase on the tube side required very small pressure differential between the two phases. It would be useful to study the reactive back extraction rate of solutes such as phenol with reversible reaction (Reed et al., 1987).

Acknowledgment

Microporous hydrophobic polypropylene flat films, X-20 hollow fibers, and the high surface area X-10 fiber Liqui-Cel module were provided by Robert W. Callahan of Hoechst Celanese Separations Products Division, Charlotte, NC. Nylon 6 flat films and hollow fibers were provided by Sigi Oberlaender of Enka America Inc., Technical Membranes Group, Asheville, NC.

Notation

a = area per unit volume of MHF module, cm^{-1}
A = area, cm^2
C_{Ao}, C_{Aw} = concentration of phenol in organic, aqueous phase, mol/cm^3
C_{Bw} = concentration of sodium hydroxide in aqueous phase, mol/cm^3
ΔC_{LM} = logarithmic mean concentration driving force, mol/cm^3
ΔC_{AM} = arithmetic mean concentration driving force, mol/cm^3
d_i = inner diameter of a hollow fiber, cm
d_o = outer diameter of a hollow fiber, cm
d_{lm} = log mean diameter of a hollow fiber, cm
D_h = hydraulic diameter of the shell side of MHF module, cm
D_{Ao}, D_{Aw} = diffusion coefficient of phenol in organic, aqueous phase, cm^2/s
D_{Bw} = diffusion coefficient of sodium hydroxide in aqueous phase, cm^2/s
k_{mo}, k_{mw} = membrane transfer coefficient for hydrophobic, hydrophilic membrane, cm/s
k_{os} = organic phase film transfer coefficient for organic flow on shell side of MHF module, cm/s
k_{wt} = aqueous phase film transfer coefficient for aqueous flow on tube side of MHF module, cm/s
K_o, K_w = overall mass transfer coefficient based on organic phase, aqueous phase, cm/s
L = length of MHF module, cm
m_i = phenol distribution coefficient between organic and aqueous phase, C_{Ao}/C_{Aw}, $(gmol/cm^3)/(gmol/cm^3)$
N_A = mass flux, $mol/cm^2 \cdot s$
N_{Gz} = Graetz number, $\pi d_i N_{Re} N_{Sc}/4L$
N_{Re} = Reynolds number, $d_i v/\eta$ or $D_h v_e/\eta$

N_{Sc} = Schmidt number, η/D_{Ao}
N_{Sh} = Sherwood number, $K_o d_i/D_{Ao}$, $K_o D_h/D_{Ao}$
Q_{aq} = aqueous flow rate, cm^3/s
Q_{org} = organic flow rate, cm^3/s
t = thickness of membrane, cm
v = velocity, cm/s
v_e = velocity, based on empty shell cross-sectional area, cm/s

Greek letters

ϵ_m = porosity of membrane
τ_m = tortuosity of membrane
η = kinematic viscosity, cm^2/s

Subscripts

m = membrane phase
o = organic phase
w = aqueous phase
e = empty cross section
t = total

Superscripts

$'$ = critical
o = initial
$*$ = dimensionless
p = location of zero caustic concentration

Literature Cited

Alexander, P. R., and R. W. Callahan, "Liquid-Liquid Extraction and Stripping of Gold with Microporous Hollow Fibers," *J. Mem. Sci.*, **35,** 57 (1987).

Astarita, G., *Mass Transfer with Chemical Reaction,* Elsevier, Amsterdam (1967).

Borwankar, R. P., C. C. Chan, D. T. Wasan, R. M. Kurzeja, Z. M. Gu, and N. N. Li, "Analysis of the effect of Internal Phase Leakage on Liquid Membrane Separations," *AIChE J.*, **34**(5), 753 (1988).

Cahn, R. P., and N. N. Li, "Separation of Phenol from Waste Water by Liquid Membrane Technique," *Sep. Sci.*, **9**(6), 505 (1974).

Callahan, R. W., "Novel Uses of Microporous Membranes: A Case Study," *AIChE Symp. Ser.*, **84**(261), 54 (1988).

Cooney D. O., and Chi-Lem Jin, "Solvent Extraction of Phenol from Aqueous Solution in a Hollow-Fiber Device," *Chem. Eng. Commun.*, **37,** 173 (1985).

Dahuron, L., and E. L. Cussler, "Protein Extraction with Hollow Fibers," AIChE J., **34**(1), 130 (1988).

Dekker, M., K. Van't Riet, J. M. G. M. Wijnans, J. W. A. Baltussen, B. H. Bijsterbosch, and C. Laane, "Membrane Based Liquid/Liquid Extraction of Enzymes Using Reversed Micelles," *Inter. Cong. of Mem. and Mem. Proc., Japan,* 15-OA 1210, 793 (1987).

D'Elia, N. A., L. Dahuron, and E. L. Cussler, "Liquid-Liquid Extraction with Microporous Hollow Fibers," *J. Mem. Sci.*, **29,** 309 (1986).

Frank, G. T., and K. K. Sirkar, "Alcohol Production by Yeast Fermentation and Membrane Extraction," *Biotecnol. Bioeng. Symp. Ser.*, **15,** 621 (1985).

———, "An Integrated Bioreactor-Separator: *In situ* Recovery of Fermentation Products by a Novel Dispersion-free Solvent Extraction Technique," *Biotecnol. Bioeng. Symp. Ser.*, **17,** 303 (1986).

Grosjean P. R. L., and H. Sawistowski, "Liquid/Liquid Mass Transfer Accompanied by Instantaneous Chemical Reaction," *Trans. Inst. Chem. Eng.*, **58,** 59 (1980).

Halwachs W., E. Flaschel, and K. Schügerl, "Liquid Membrane Transport—A Highly Selective Separation Process for Organic Solutes," *J. Mem. Sci.*, **6,** 33 (1980).

International Critical Tables of Numerical Data, Physics, Chemistry and Technology, **V**, 67 (1929).

Jauernik, R., "Neuere Entwicklung beim Phenosolvan-Verfahren," *Erdöl und Kohle,* **13,** 252 (1960).

Kiani, A., R. R. Bhave, and K. K. Sirkar, "Solvent Extraction with Immobilized Interfaces in a Microporous Hydrophobic Membrane," *J. Mem. Sci.*, **20,** 125 (1984).

Lanouette, K. H., "Treatment of Phenolic Wastes," *Chem. Eng.* (Deskbook Issue), **84**(22), 99 (1977).

Prasad, R., "Dispersion-Free Solvent Extraction Through Microporous Membranes," Ph.D. Thesis, Stevens Inst. Techol., Hoboken, NJ (1986).

Prasad, R., and K. K. Sirkar, "Microporous Membrane Solvent Extraction," *Sep. Sci. Tech.*, **22**(2,3), 619 (1987a).

———, "Solvent Extraction with Microporous Hydrophilic and Composite Membranes," *AIChE J.*, **33**(7), 1057 (1987b).

———, "Dispersion-Free Solvent Extraction with Microporous Hollow-Fiber Modules," *AIChE J.*, **34**(2), 177 (1988).

Prasad, R., R. R. Bhave, A. Kiani, and K. K. Sirkar, "Further Studies on Solvent Extraction with Immobilized Interfaces in a Microporous Hydrophobic Membrane," *J. Mem. Sci.*, **26,** 79 (1986).

Prasad, R., G. T. Frank, and K. K. Sirkar, "Nondispersive Solvent Extraction Using Microporous Membranes," *AIChE Symp. Ser.*, **84**(261), 42 (1988).

Reed, D. L., A. L. Bunge, and R. D. Noble, "Influence of Reaction Reversibility on Continuous-Flow Extraction by Emulsion Liquid Membranes," *Am. Chem. Soc. Symp. Ser.*, No. 347, 62 (1987).

Sengupta, A., R. Basu, R. Prasad, and K. K. Sirkar, "Separation of Liquid Solutions by Contained Liquid Membranes," *Sep. Sci. Tech.*, **23**(12,13), 1735 (1988a).

Sengupta, A., R. Basu, and K. K. Sirkar, "Separation of Solutes from Aqueous Solutions by Contained Liquid Membrane," *AIChE J.*, **34**(10), 1698 (1988b).

Skelland, A. H. P., *Diffusional Mass Transfer,* Wiley, New York (1974).

Terry, R. E., N. N. Li, and W. S. Ho, "Extraction of Phenolic Compounds and Organic Acids by Liquid Membranes," *J. Mem. Sci.*, **10,** 305 (1982).

Wilke, C. R., and P. Chang, "Correlation of Diffusion Coefficients in Dilute Solutions," *AIChE J.*, **1**(2), 264 (1955).

Won, K. W., and J. M. Prausnitz, "Distribution Coefficient of Phenolic Solutes between Water and Organic Solvents," *J. Chem. Thermody.*, **7,** 661 (1975).

Yang, M. C. and E. L. Cussler, "Designing Hollow-Fiber Contactors," *AIChE J.*, **32,** 1910 (1986).

Manuscript received Dec. 22, 1988, and revision received Jan. 17, 1990.